Journal of the Mechanical Behavior of Biomedical Materials 92 (2019) 137–143

Contents lists available at ScienceDirect

Journal of the Mechanical Behavior of Biomedical Materials

journal homepage: www.elsevier.com/locate/jmbbm

Friction in the contact between skin and a soft counter material: Effects of hardness and surface finish

M. Klaassen[a], E.G. de Vries[a], M.A. Masen[b,*]

[a] Department of Engineering Technology, University of Twente, the Netherlands
[b] Department of Mechanical Engineering, Imperial College London, United Kingdom

A B S T R A C T

The interaction behaviour of skin with a counter surface depends strongly on the surface roughness of the counter surface. For relatively hard surfaces this effect is described in various literature, but for soft, or compliant, materials this is much less studied. Inside the contact, the protuberances on the surface will deform substantially. In order to gain insights into the effect of surface roughness and hardness on the frictional behaviour between skin and a soft counter surface a range of experiments were performed using artificial skin and various silicone compounds which are commonly used in medical devices that interact with the human skin. Using these results, a 'friction map' was created that shows the friction behaviour as a function of the elastic modulus and the surface roughness. When the surface roughness is increased the friction coefficient decreases due to the reduction in the real area of contact, which weakens the adhesion between the two surfaces. A minimum coefficient of friction was observed at a surface roughness of approximately 4 μm. For the softest compounds tested there was minimal effect of surface roughness on friction because the roughness protuberances inside the contact will be flattened. Silicone compounds with increased hardness showed a larger sensitivity of the friction to the surface roughness, because these harder surface roughness protuberances are more resistant against deformation. The friction map provides a tool when designing products that require certain frictional properties: for products that are required to adhere to skin a smooth and soft material is recommended, whereas for products that require a low coefficient of friction a harder compound with a surface roughness of approximately 4 μm is recommended.

1. Introduction

Many medical devices that are designed to interact with human skin or other soft biological tissue employ a soft polysiloxane ('*silicone*') material to act as the interface with the skin. Examples include face masks, such as for continuous positive airway pressure therapy, medical tubing, prosthetic liners as well as soft tissue implants (Sanders et al., 2004; Sanders et al., 1992; Bałazy et al., 2006; Barr and Bayat, 2011). The compliance of the silicone material increases the contact area between the skin and the counter surface and thus reduces the contact pressure and as a result may provide a perception of increased comfort. However, the large area of contact combined with the tackiness of the silicone, particularly at elevated levels of temperature and moisture due to occlusion inside the contact, may create a harsh environment for the skin in which elevated levels of shear can easily lead to irritation and damage in the form of wounds, blisters or ulceration (Laszczak et al., 2016; De Wert et al., 2015; Guerra and Schwartz, 2011; Derler et al., 2012; Klaassen et al., 2016; Bader et al., 2005).

The work presented in this paper is based on the concept that tissue damage caused by the severity of the contact during interaction with silicone-based medical devices may be reduced by reducing the shear stresses acting on the tissue (De Wert et al., 2015; Derler et al., 2012; Linder-Ganz and Gefen, 2007). This can be done either globally, i.e. by reducing the overall level of shear in the contact or, in cases where a certain amount of shear is required for appropriate function, by transferring the shear loading to skin sites that are more tolerant to loading and thus unloading more sensitive skin sites. For example for a transtibial amputation the sensitive areas of the skin that should not be loaded include the patella, tibial crest and bony prominences such as the fibular head (Lee et al., 2005). In this work, we study the effects of changing the surface roughness and the hardness of silicone surfaces that are in contact with the skin. This leads to a set of 'design criteria' for applications where friction is important when two soft bodies are in contact.

1.1. Contact and friction in skin contacts

It is well known that for skin-object interactions, just like most other tribological contacts, both the material properties and the surface finish will affect the friction, see e.g. Zum Gahr (1987). Typically, the friction observed in skin contacts shows an inverse relationship with the surface roughness of the counter body. Hendriks et al. showed that the coefficient of friction for skin interacting with a metal surface reduced by approximately an order of magnitude when the metal's roughness increased from 0.1 μm to 10 μm (Hendriks and Franklin, 2009). Masen observed a similar trend for the dry index finger against stainless steel,

* Corresponding author.
E-mail address: m.masen@imperial.ac.uk (M.A. Masen).

https://doi.org/10.1016/j.jmbbm.2019.01.006
Received 5 September 2018; Received in revised form 8 January 2019; Accepted 9 January 2019
Available online 10 January 2019
1751-6161/

with the coefficient of friction steadily decreasing from 0.9 for a surface with an Rq of 0.004 μm to 0.4 for an Rq of 1.8 μm (Masen, 2011). However, for wet skin an increased coefficient of friction was found for intermediate surface roughness values, which was attributed to the combined effects of adhesion and deformation. Derler et al. compared the coefficient of friction for smooth and rough glass against the ulnar side of the hand and observed lower coefficients of friction for the rougher counter surface (Derler et al., 2009). Baum et al. studied the effect of surface roughness between a snake skin replica and a glass counter surface and observed a decrease in coefficient of friction for increasing roughness up to a Ra of 9 μm, after which the coefficient of friction increases with increasing roughness (Baum et al., 2014). This means that controlled local variations of the friction, and thus the resulting shear stress acting on the skin may be achieved by developing surfaces with local variations of material properties and/or surface finishing. However, at present, one of the limiting factors in developing such products is that the contact between skin and silicone is a combination of two compliant materials, whereas the majority of studies investigating the tribology of skin have focused on the interaction of skin with materials that have a significantly higher stiffness. This means that in most studies the deformation of the counter surface can be ignored and only the deformation of the skin is taken into account. In the case of a contact between the skin and a compliant silicone product, such as a prosthetic liner or a face mask, this assumption cannot be made as both the skin and the counter surface have comparable stiffness. The objective of the current work is to investigate the frictional forces in the contact between skin and a soft counter body, and how they relate to the stiffness (or compliance) and the surface roughness of the silicone surface.

2. Methods

2.1. Skin mimic

The frictional behaviour of in-vivo skin has been studied by various researchers, recent examples include Klaassen et al., 2016; Klaassen et al., 2017; Hendriks and Franklin, 2009; Masen, 2011; Derler et al., 2009; Adams et al., 2007; Tomlinson et al., 2009; Zahouani et al., 2009; Leyva-Mendivil et al., 2017; van Kuilenburg et al., 2013; Veijgen et al., 2013. Although many of the underlying mechanisms are still not understood to a level that predictive quantitative models can be developed, a common conclusion is that whilst measurement results obtained on healthy subjects show a large spread as a result of both inter- and intra-subject variability (Cua et al., 1990; Veijgen et al., 2012), discernible qualitative trends can be obtained. To limit the dependence on test subjects and facilitate investigating trends, various studies have reported on the development of tribological mimics for skin. Such mimics range from fairly simple elastomers to complex multi-layered structures with tailored bulk- and surface properties (Nachman and Franklin, 2016; Morales Hurtado et al., 2016). Derler and co-workers (Derler et al., 2007; Cottenden and Cottenden, 2013; Falloon and Cottenden, 2016) investigated the use of an 'artificial leather' (Lorica Soft, Italy) as a tribological skin mimic and concluded that this material provides friction results that are representative for data obtained in-vivo.

For the current study, the availability of a suitable skin mimic eliminates the need for performing experiments on volunteers, and indeed testing on a skin mimic is preferred as it will reduce variability and thus improve the repeatability of the results, which enables distinguishing trends that would not be discernible from results obtained on life subjects. Fig. 1 shows confocal microscopy images of a representative in-vivo skin specimen, measured on the volar forearm and the Lorica Soft skin mimic used in this study. The measured roughness value (Ra) of the two specimens are similar, and both surfaces show somewhat comparable texture, although the micro relief on the skin shows a larger number of furrows, which are also more strongly defined. This can be observed by the triangular pattern on the real skin surface which are separated by sharp edges. The artificial skin also contains furrows, but these have smoother edges and the microrelief features are larger.

The reduced Young's modulus $E^* = E/(1-\nu^2)$ of the skin mimic, as determined by fitting a Hertz (elastic) contact model through spherical indentation data, is 1.8 MPa. This value corresponds well with the elastic modulus of 1.5 MPa for the epidermis as reported in the review paper by van Kuilenburg et al. (2012).

2.2. Silicone specimens

Silicone test specimens were produced using tin-cured silicone compounds (Smooth-On, Pennsylvania, USA) by casting into hemispherical moulds. The specimens are hemispheres with a diameter of 8.0 mm, which were glued onto aluminium sample holders. Specimens with different compliances are obtained by using three different silicone compounds. The Young's moduli for the specimens were determined by performing indentation experiments on a UMT Tribolab system (Bruker, USA). Additionally, Shore A Hardness values were measured using a hardness tester (Zwick, Germany). The viscoelastic characteristic of the materials, as represented by the ratio between storage and loss modulus, $\tan(\delta)$ was determined by performing dynamic-mechanical analysis (DMA) measurements on a Metravib VA2000 system (Metravib, France). The obtained mechanical values are reported in Table 1. For each silicone compound, seven samples are produced with Ra roughness values ranging between 0.5 μm and 7.8 μm, as measured using a confocal microscope (Keyence, Japan). The range of roughness values was achieved using moulds with varying surface roughness. As the surface roughness of a moulded specimen is not simply a mirror-copy of the mould but also depends on material properties such as the viscosity of the silicone compound, the specimens of the different compounds made in the same mould have a comparable, but not 100% identical, surface roughness. Fig. 2 shows images of three representative silicone specimens, 'smooth', 'medium' and 'rough' used in this study.

Contact angle measurements were performed using three liquids; n-hexane, glycerol and water, from which the surface free energy was calculated using the method of Owens and Wendt (1969). The surface free energy of the three compounds was between 26 and 27 mJ/m^2 and did not significantly differ between the three compounds. Therefore, it may be assumed that the interaction of all three silicone materials in terms of the interfacial shear strength (τ) is constant and any observed differences in contact behaviour follow from differences in the real contact area between the two interacting surfaces. The characteristics of the various specimens are summarised in Table 1.

2.3. Friction measurements

Friction measurements are performed on an UMT Tribolab system (Bruker, USA). A spherical silicone pin is used as the upper specimen, whilst the flat skin mimic is the bottom specimen. Contact is initiated by lowering the spindle-driven vertical stage that contains the silicone specimen at a speed of 10 $\mu m\,s^{-1}$. The skin specimen is mounted on a horizontal linear drive that, after contact is established, starts moving at a speed of 100 $\mu m\,s^{-1}$ to create a sliding contact. Both the applied normal force and the resulting friction force are measured using the Bruker DFM-2.0 two-directional force transducer. The resolution of this force transducer in both normal and lateral direction is 1.0 mN. Force readings are recorded at 1000 Hz and filtered using a moving average filter with a width of 10 samples.

Experiments were performed under room conditions (22 °C, 60% RH) at six normal loads, ranging between 0.04 N and 1.28 N, resulting in Hertz mean contact pressures of approximately 27 kPa to 210 kPa. These values are clinically relevant as they represent typical pressures found at the interface of a lower limb stump and a prosthetic liner, and

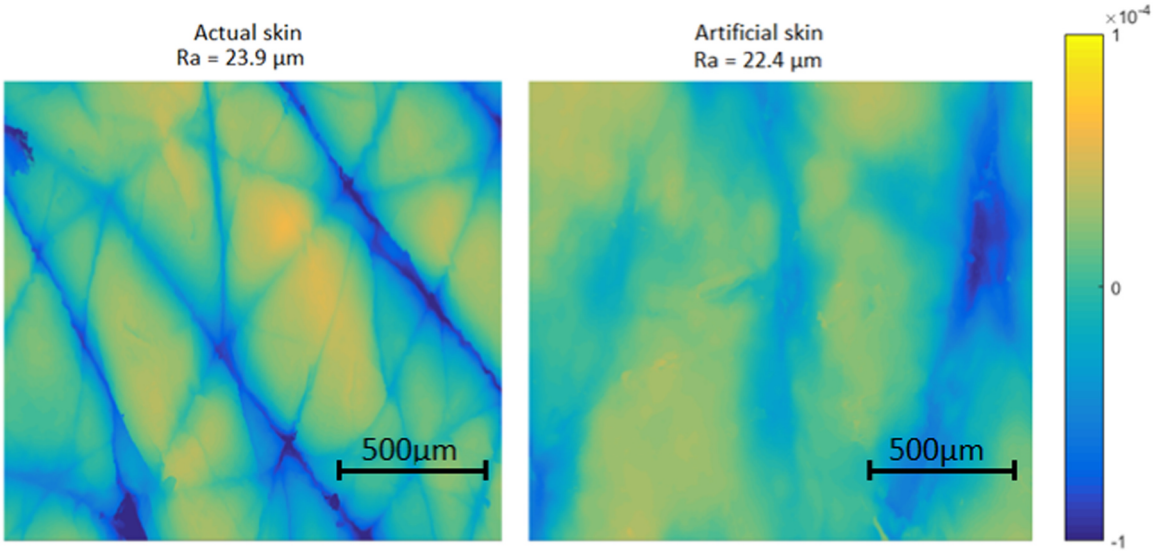

Fig. 1. Confocal microscopy images of in-vivo skin (left) as well as the skin mimic employed in this study (right).

Table 1
Properties of the silicone specimens.

		Soft compound	Medium compound	Hard compound
Specimen shape		Hemisphere		
Specimen radius of curvature [mm]		4.0		
E-Modulus [MPa]		0.45	0.60	0.91
Approximate Shore Hardness [Shore A]		3.6	10.4	19.2
Viscoelastic loss tangent, tan(δ) [-]		0.08	0.04	0.04
Surface Free Energy [mJ/m^2]		26.9	26.2	27.1
Roughness Ra [µm]	**Specimen A ('smooth')**	0.7	0.5	0.7
	Specimen B	0.9	1.1	1.0
	Specimen C	1.0	1.2	1.3
	Specimen D ('medium')	2.3	1.9	2.3
	Specimen E	2.8	3.3	4.2
	Specimen F	3.9	5.9	5.9
	Specimen G ('rough')	7.0	6.6	7.8

are somewhat lower than the peak pressures reported in (Lee et al., 2004). A stroke length of 10 mm was sufficient to initiate full macroscopic sliding even for the most compliant compound at the highest applied load. The skin-product interface for most silicone-based products, such as face masks and prosthetic liners, is stationary or static contact meaning that macroscopic sliding does not occur. The maximum static coefficient of friction ($\mu_{s,max}$) is therefore an important factor determining the shear forces that may occur in the skin, and is the parameter of interest in this study. It defines the transition between sticking (i.e. static friction) and rubbing (i.e. dynamic friction) in the contact between the silicone and the skin. Experimentally, moving the specimens at a speed of 100 µm/s facilitates observing a clear transition between the static and dynamic friction regimes.

Each measurement consists of two back-and-forth reciprocating motions and each measurement is performed three times, resulting in a total of 12 values for $\mu_{s,max}$ measured around the reciprocation points per experimental condition.

Typical measured force signals are shown in Fig. 3: the dark green line shows the applied normal force, whilst the dark blue line shows the measured friction force F_f. The graph also shows the second time derivative of the average filtered friction force, $\ddot{F}_f$, which can be used to identify the onset of full macroscopic sliding. It is interesting to note that the obtained friction force signal is quite 'square' and no static friction peak at the reciprocal point is observed. The maximum static friction force is therefore defined as the maximum friction force measured within the first 100 µm after initiation of full sliding. Both the

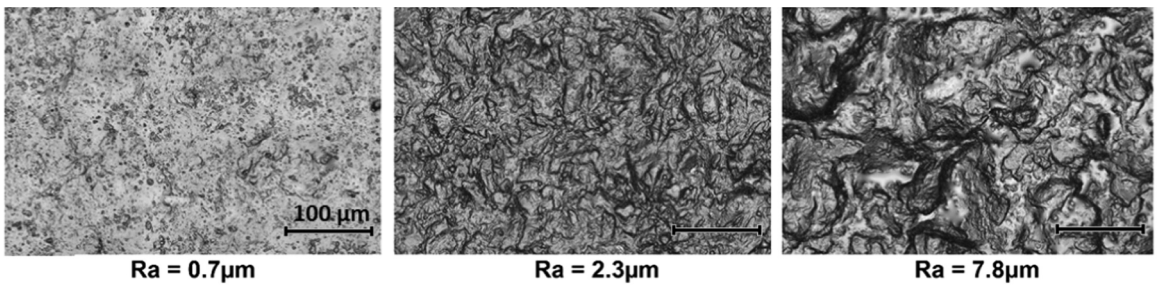

Fig. 2. Microscope images of the smooth (Ra = 0.7 µm), medium (Ra = 2.3 µm) and rough (Ra = 7.8 µm) silicone specimens. The bar represents 100 µm, each image shown at the same scale.

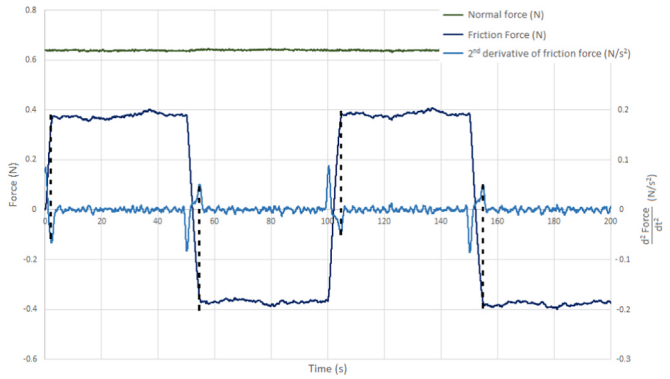

Fig. 3. A typical force measurement. The dark green line shows the applied load, which is fairly constant at 0.64 N. The dark blue line shows the resulting friction force, alternating between 0.4 N and -0.4N with each reciprocating motion. The second time derivative of the friction force is shown in light blue. A local extreme in this calculated signal indicates indicates the transition to full macroscopic sliding. (For interpretation of the references to color in this figure legend, the reader is referred to the web version of this article.).

static coefficient of friction (calculated as the peak static friction force divided by the normal load) and the absolute peak static friction force are used for further analysis.

3. Results

Fig. 4(a)–(c) and 5(a)–(c) show the combined results from the friction measurements. The three different graphs represent (a) the soft, (b) the medium and (c) the hard compound.

3.1. Normal load effects

Fig. 4(a), (b) and (c) show the maximum coefficient of static friction as a function of the applied normal force for all samples. The different shades of the data points represent the various roughness values of the silicone specimens. The coefficient of friction decreases strongly with increasing normal load. The dashed lines indicate the trends observed for the highest and lowest friction values, these represent the smoothest and roughest specimen respectively. Particularly at the lower end of the applied loads, there is a substantial difference between the maximum and minimum measured coefficients of friction. This difference in coefficient of friction at low loads is already quite pronounced for the softer silicone and is even larger for the with silicone compounds with higher stiffness or shore hardness. At increased loads the difference between the various rough specimens reduces for all compounds. A logical explanation is that at low loads the in-contact, or deformed roughness of the silicone surface persists, particularly for the harder compounds, whilst at the higher loads the roughness asperities on all the silicone surface are deformed, creating what is, in essence, a smooth contact.

3.2. Roughness effects

The graphs in Fig. 5 show the same data as Fig. 4, but now represented as a function of the surface roughness of the specimens. To enable differentiation between the curves for the various applied loads in these graphs, the data is represented in terms of the maximum static friction force and not the coefficient of friction, whilst the y-axis has a logarithmic scale. Particularly for the harder silicone compound the roughness of the silicone has a major effect on the maximum friction in the contact, and therefore at the stresses at the onset of sliding. The

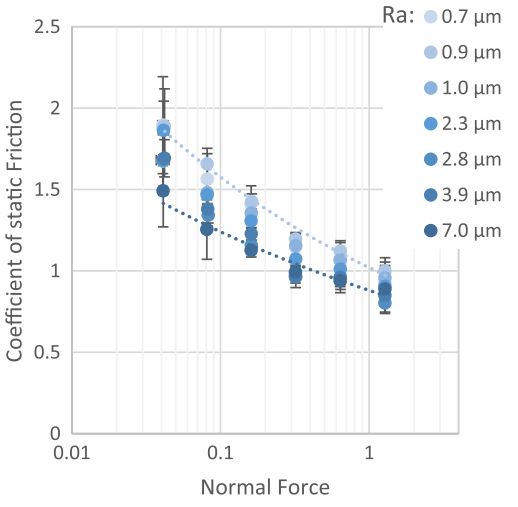

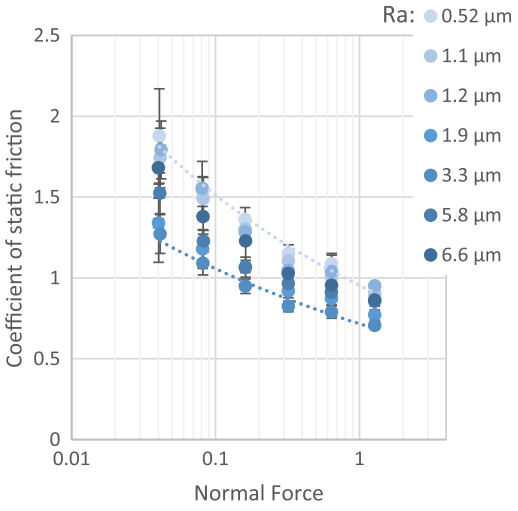

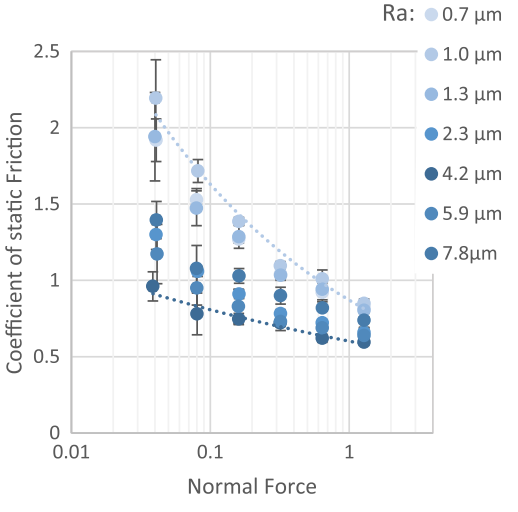

Fig. 4. The maximum static coefficient of friction as a function of the normal load for the A) soft, B) medium and C) hard silicone specimens. The legend shows the ra surface roughness values.

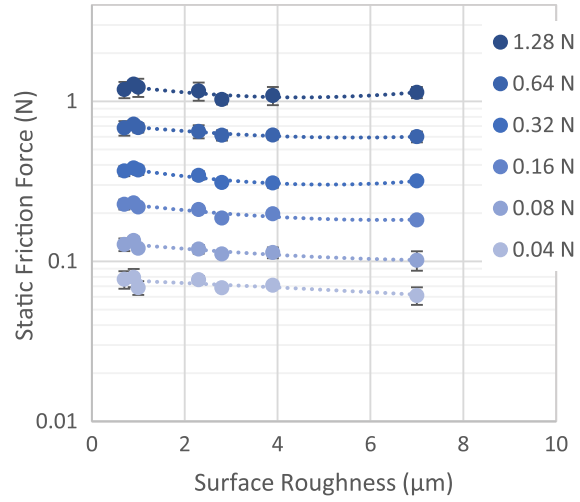

(A) SOFT SILICONE

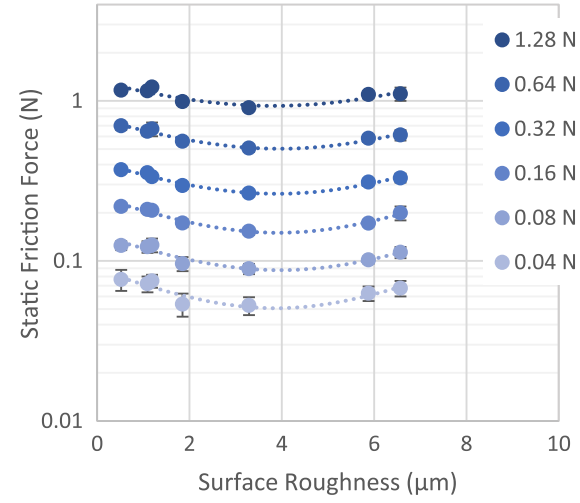

(B) MEDIUM SILICONE

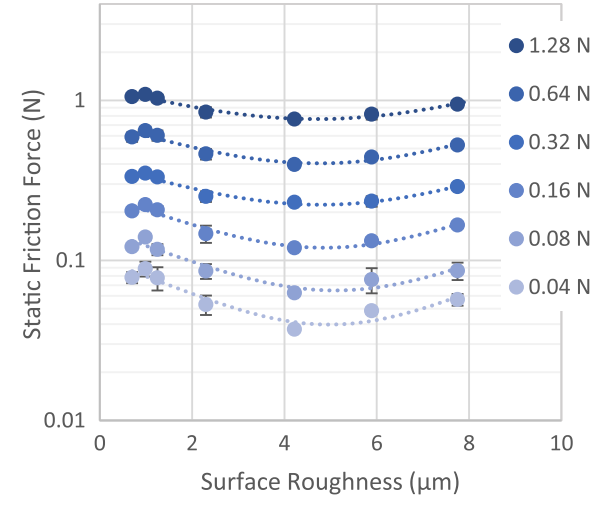

(C) HARD SILICONE

Fig. 5. The peak static friction force as a function of the surface roughness for different normal loads for A) the softest compound, B) medium compound and c) hardest compound.

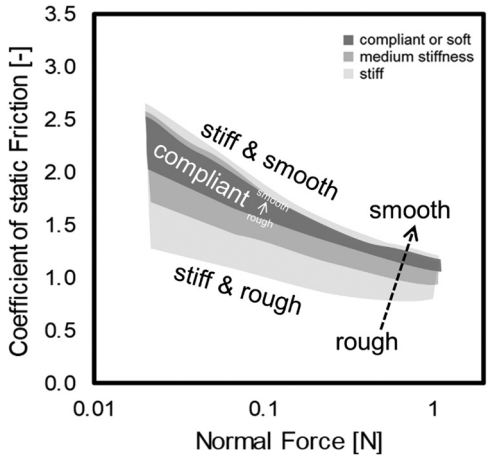

Fig. 6. Schematic overview of all results, superimposed.

friction forces are relatively high at both the smooth and rough-end of the range, with a minimum friction observed for intermediate roughness values. This is particularly evident for the medium and harder silicone compounds and is clearly shown by the dotted lines in the graphs, which are second order polynomial fits through the data points. These curves indicate that a minimum friction occurs at a roughness Ra between 4 and 5 µm. Additionally, the curvature of the fitted curves increases with compound stiffness, indicating that stiffer or harder materials show a more pronounced effect of surface roughness on friction.

4. Discussion

From the obtained experimental results some general trends can be deduced which allows to hypothesize on the predominant mechanisms underlying the interaction behaviour. In the following discussion one needs to keep in mind that, even though terms such as 'compliant' and 'stiff' are used, these refer to silicone surfaces with Shore A hardness values ranging between 3 and 20, meaning all materials in this study are rather soft or compliant in comparison to the stratum corneum and the skin mimic used in this study.

Fig. 6 shows a schematic overview in which all previously presented results are superimposed. The figure shows that the static friction values obtained between the skin mimic and silicone materials are high, ranging from 1 to 3. Additionally:

- The static coefficient of friction measured at low loads is much higher than for higher loads
- For rough surfaces a lower static friction is found than for smooth surfaces.
- For stiff materials the static friction values are strongly sensitive to the surface roughness. This roughness effect is particularly pronounced at low loads. In contrast, the static friction for compliant materials is fairly insensitive to the surface roughness.
- For smooth surfaces the effect of stiffness of the material is fairly small: the static friction obtained with the smooth compliant silicones is at a similar level as the smooth stiff silicones. With increasing loads this trend continues: the compliant silicone contacts have a friction level similar to the smooth stiffer materials, but at increased loads the size of the 'envelope' in which all results fit is strongly reduced, and the coefficient of friction appears to approach a single asymptotic value of about $\mu \approx 1$.

The static friction in the contact between two compliant bodies, such as the silicone component and the skin surrogate used in the present study, follows from combination of adhesive friction and roughness interlocking mechanisms. The adhesion results from shearing of physical bonds, such as Van der Waals forces and is the product of the interfacial shear strength of the sliding interface and the area of contact between the two materials. The observed reduction of the coefficient of friction with increasing applied force is commonly linked to adhesion being the dominating friction mechanism.

In the presented results, however, because the difference in surface free energy between the silicone specimens employed in this study is negligible, the shear strength of the skin-silicone interface can be assumed to be identical for all specimens and any differences in adhesive friction force are only determined by the area of contact between the two materials. The implication of this would be that, if the frictional behaviour of the contact was only determined by adhesion, the friction of the compliant material should be higher than that of the stiff material. This is not the case, indicating that adhesion is not the sole mechanism and that interlocking of roughness asperities also plays an important role. Indeed, for smooth surfaces the observed friction for the compliant and the stiff material are similar.

For surfaces with increased roughness, the roughness protuberances for a compliant material are more easily deformed and compressed than those on a stiff surface, causing a significant difference in friction at the lower end of the loading scale. At increased loads the surface roughness for all specimens is compressed and we obtain a 'smooth contact' where the measured coefficient of friction for all specimens appears to converge.

Fig. 6 showed that for smooth surfaces, the friction force decreases with increasing roughness, while for rough surfaces the friction increases with increasing roughness. For the surfaces with a fairly high elastic modulus, a minimum friction was obtained for surface roughness values of approximately Ra $\approx$ 4 μm whilst for the more compliant surfaces the minimum friction occurs at Ra $\approx$ 6 μm. Depending on the stiffness of the silicone, roughness protuberances or asperities inside the contact will be compressed to a certain degree and it is hypothesized that a surface roughness of approximately 5 μm is large enough to not be fully compressed in the contact. This means that friction reaches a minimum because of the combination of a reduced real area of contact between the silicone specimen and the skin mimic in combination with minimal effects of roughness interlocking. This agrees with previous findings, see e.g. Hendriks and Franklin (2009) and Gee et al. (2005). For skin in contact with a range of engineering materials, i.e. materials with a Young's modulus at least an order of magnitude higher, Hendriks suggests that the surface roughness at which the minimum dynamic coefficient of friction occurs is expected to increase with increasing Young's modulus. Gee et al. reported the minimum friction coefficient for a finger sliding against steel to occur at a surface roughness of 3.2 μm. However, next to skin against hard surfaces, these studies relate to dynamic friction where visco-elastic effects may also play a role. In addition, the friction ridges on the finger might introduce a further effect of ploughing or mechanical interlocking, meaning that these results cannot simply be translated to the current situation under study. It should be noted that the silicone compounds used in the present study only covered three different stiffness values, meaning there is insufficient detail to determine whether there is a true significant effect of the elastic modulus on the surface roughness at which the friction force shows a minimum.

The results obtained in the present paper can be diagrammatically summarised into a design graph for soft-skin contacts, shown in Fig. 7. This diagram shows the coefficient of friction as a function of both the surface roughness and the elastic modulus, taking into account the boundaries of the present study, i.e. three different elastic moduli, between 0.45 and 0.9 MPa were employed in this study, with roughness values ranging between 0.7 μm and 8 μm and contact pressures between 27 and 210 kPa. These boundaries cover the range of practically relevant materials, roughness values and conditions. The figure is composed by combining the second order polynomial fits that were presented in Fig. 4(a)–(c) into one figure, interpolating between the three stiffnesses. The colours in the diagram indicate the value of the coefficient of friction. The diagram provides an overview of the combined effects of surface roughness and elastic modulus (or shore hardness) and indicates which properties to focus on or select when designing a material and surface with a certain desired friction behaviour. This graph clearly shows that there is a combination of a surface roughness and a Young's modulus where the shear forces acting on the skin will be minimal.

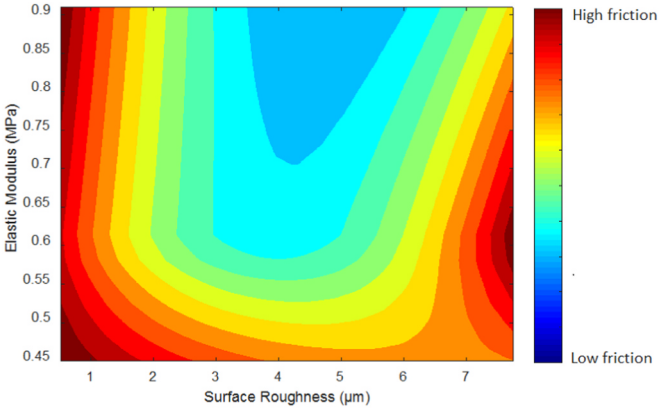

Fig. 7. Friction coefficient map for surface roughness and elastic modulus.

5. Conclusions

This paper discussed the effects of the surface roughness and the compliance (quantified in terms of elastic modulus or shore hardness) of soft silicone compounds in contact with a mimic material for human skin. In such systems, friction is relatively high for both smooth surfaces (i.e. a roughness Ra < 1 μm) and rough surfaces (Ra > 6 μm), with a minimum friction found for surfaces with a roughness Ra $\approx$ 5 μm. The initial reduction of the coefficient of friction when increasing the surface roughness for smooth surfaces is attributed to a reduction of the real area of contact, whereas the subsequent increase of the friction with further increasing surface roughness is attributed to the interlocking of roughness asperities. Soft materials only show a minor effect of surface roughness as the roughness asperities are easily compressed and the in-contact surface roughness is smooth, whereas for the stiffer silicone compound the in-contact surface roughness is more persistent, although this persistence strongly depends on the applied load.

For the studied contact between a skin mimic and silicone materials, the relative sensitivity of the friction to the roughness and the stiffness of the silicone is:

- At low surface roughness the effect of changing the surface roughness is large: the friction decreases with increasing roughness. For these roughness values the effect of changing the elastic modulus is almost negligible.
- For intermediate surface roughness values the friction becomes much more sensitive to the elastic modulus. At roughness values between 3 and 6 μm the friction is only affected by the elastic modulus of the silicone material. Increasing the elastic modulus reduces the friction in the contact.
- At the higher end of the surface roughness the sensitivity changes again, showing the friction is affected strongly by the surface roughness and only to a minor degree by the elastic modulus of the material. An increasing roughness results in increasing friction, with an elevated friction for the softer materials.

When designing a product that has soft surfaces intended to interact with the skin and where shear forces resulting from (static) friction plays an important role, these guidelines can help selecting a combination of surface roughness and material to optimise the product. For a product this could mean that skin areas that are prone to overloading or damage by shear forces can be relieved by choosing a surface roughness that is close to 4 μm, or by locally using a less compliant material. Skin areas that are sensitive to irritation or damage due to rubbing (dynamic friction) would benefit from locally using a softer material to ensure sticking. This would enable optimisation of the local friction condition using a combination of surface techniques.

Acknowledgements

This research was supported by the Netherlands Organisation for Scientific Research (NWO) under grant number OT-12673.

References

Adams, M.J., Briscoe, B.J., Johnson, S.A., 2007. Friction and lubrication of human skin. Tribol. Lett. 26 (3), 239–253.
Bader, D., Bouten, C., Colin, D., Oomens, C., 2005. Pressure Ulcer Research. Springer-Verlag, Berlin/Heidelberg.
Bałazy, A., Toivola, M., Reponen, T., Podgórski, A., Zimmer, A., Grinshpun, S.A., 2006. Manikin-based performance evaluation of N95 filtering-facepiece respirators challenged with nanoparticles. Ann. Occup. Hyg. 50 (3), 259–269.
Barr, S., Bayat, A., 2011. Breast surgery review article: breast implant surface development: perspectives on development and manufacture. Aesthetic Surg. J. 31 (1), 56–67.
Baum, M.J., Heepe, L., Fadeeva, E., Gorb, S.N., 2014. Dry friction of microstructured polymer surfaces inspired by snake skin. Beilstein J. Nanotechnol. 5 (1), 1091–1103.
Cottenden, D.J., Cottenden, A.M., 2013. A study of friction mechanisms between a surrogate skin (Lorica soft) and nonwoven fabrics. J. Mech. Behav. Biomed. Mater. 28, 410–426.
Cua, A.B., Wilhelm, K.P., Maibach, H.I., 1990. Friction properties of human skin: relation to age, sex and anatomical region, stratum corneum hydration and trensepidermal water loss. Skin. Pharmacol. Physiol. 123 (4), 473–479.
De Wert, L.A., Bader, D.L., Oomens, C.W.J., Schoonhoven, L., Poeze, M., Bouvy, N.D., 2015. A new method to evaluate the effects of shear on the skin. Wound Repair Regen. 23 (6), 885–890.
Derler, S., Schrade, U., Gerhardt, L.C., 2007. Tribology of human skin and mechanical skin equivalents in contact with textiles. Wear 263 (7–12), 1112–1116.
Derler, S., Gerhardt, L.C., Lenz, A., Bertaux, E., Hadad, M., 2009. Friction of human skin against smooth and rough glass as a function of the contact pressure. Tribol. Int. 42 (11–12), 1565–1574.
Derler, S., Rao, A., Ballistreri, P., Huber, R., Scheel-Sailer, A., Rossi, R.M., 2012. Medical textiles with low friction for decubitus prevention. Tribol. Int. 46 (1), 208–214.
Falloon, S.S., Cottenden, A., 2016. Friction between a surrogate skin (Lorica Soft) and nonwoven fabrics used in hygiene products. Surf. Topogr. Metrol. Prop. 4 (3).
Zum Gahr, K.H., 1987. Microstructure and Wear of Materials, Elsevier Tribology Series. Elsevier ISBN 978-0-444-42754-0.
Gee, M.G., Tomlins, P., Calver, A., Darling, R.H., Rides, M., 2005. A new friction measurement system for the frictional component of touch. Wear 259 (7–12), 1437–1442.
Guerra, C., Schwartz, C.J., 2011. Development of a synthetic skin simulant platform for the investigation of dermal blistering mechanics. Tribol. Lett. 44 (2), 223.
Hendriks, C.P., Franklin, S.E., 2009. Influence of surface roughness, material and climate conditions on the friction of human skin. Tribol. Lett. 37 (2), 361–373.
Klaassen, M., Schipper, D.J., Masen, M.A., 2016. Influence of the relative humidity and the temperature on the in-vivo friction behaviour of human skin. Biotribology 6, 21–28.
Klaassen, M., de Vries, E.G., Masen, M.A., 2017. The static friction response of non-glabrous skin as a function of surface energy and environmental conditions. Biotribology 11, 124–131.
Laszczak, P., McGrath, M., Tang, J., Gao, J., Jiang, L., Bader, D.L., Moser, D., Zahedi, S., 2016. A pressure and shear sensor system for stress measurement at lower limb residuum/socket interface. Med. Eng. Phys. 38 (7), 695–700.
Lee, W.C., Zhang, M., Mak, A.F., 2005. Regional differences in pain threshold and tolerance of the transtibial residual limb: including the effects of age and interface material. Arch. Phys. Med. Rehabil. 86 (4), 641–649.
Lee, W.C.C., Zhang, M., Boone, D.A., Contoyannis, B., 2004. Finite-element analysis to determine effect of monolimb flexibility on structural strength and interaction between residual limb and prosthetic socket. J. Rehabil. Res. Dev. 41 (6), 775–786.
Leyva-Mendivil, M.F., Lengiewicz, J., Page, A., Bressloff, N.W., Limbert, G., 2017. Erratum to: skin microstructure is a key contributor to its friction behaviour (Tribology Letters, (2017), 65, 1, (12), 10.1007/s11249-016-0794-4). Tribol. Lett. 65 (4), 1–17.
Linder-Ganz, E., Gefen, A., 2007. The effects of pressure and shear on capillary closure in the microstructure of skeletal muscles. Ann. Biomed. Eng. 35 (12), 2095–2107.
Masen, M.A., 2011. A systems based experimental approach to tactile friction. J. Mech. Behav. Biomed. Mater. 4 (8), 1620–1626.
Morales Hurtado, M., de Vries, E.G., Zeng, X., van der Heide, E., 2016. A tribo-mechanical analysis of PVA-based building-blocks for implementation in a 2-layered skin model. J. Mech. Behav. Biomed. Mater. 62, 319–332.
Nachman, M., Franklin, S.E., 2016. Artificial skin model simulating dry and moist in vivo human skin friction and deformation behaviour. Tribol. Int. 97, 431–439.
Owens, D.K., Wendt, R.C., 1969. Estimation of the surface free energy of polymers. J. Appl. Polym. Sci. 13 (8), 1741–1747.
Sanders, J.E., Daly, C.H., Burgess, E.M., 1992. Interface shear stresses during ambulation with a below-knee prosthetic limb. J. Rehabil. Res. Dev. 29 (4), 1–8.
Sanders, J.E., Nicholson, B.S., Zachariah, S.G., Cassisi, D.V., Karchin, A., Fergason, J.R., . 2004. Testing of elastomeric liners used in limb prosthetics: classification of 15 products by mechanical performance. J. Rehabil. Res. Dev. 41 (2), 175–186.
Tomlinson, S.E., Lewis, R., Carré, M.J., 2009. The effect of normal force and roughness on friction in human finger contact. Wear 267 (5–8), 1311–1318.
van Kuilenburg, J., Masen, M.A., van der Heide, E., 2012. Contact modelling of human skin: what value to use for the modulus of elasticity? Proc. Inst. Mech. Eng. Part J. J. Eng. Tribol. 227 (4), 349–361.
van Kuilenburg, J., Masen, M.A., van der Heide, E., 2013. The role of the skin microrelief in the contact behaviour of human skin: contact between the human finger and regular surface textures. Tribol. Int. 65, 81–90.
Veijgen, N.K., Masen, M.A., van der Heide, E., 2012. Relating friction on the human skin to the hydration and temperature of the skin. Tribol. Lett. 49 (1), 251–262.
Veijgen, N.K., van der Heide, E., Masen, M.A., 2013. A multivariable model for predicting the frictional behaviour and hydration of the human skin. Skin. Res. Technol. 19 (3), 330–338.
Zahouani, H., Vargiolu, R., Boyer, G., Pailler-Mattei, C., Laquièze, L., Mavon, A., 2009. Friction noise of human skin in vivo. Wear 267 (5–8), 1274–1280.